

FGF14 modulates resurgent sodium current in mouse cerebellar Purkinje neurons

Haidun Yan^{1,2}, Juan L Pablo^{2,3}, Chaojian Wang^{1,2}, Geoffrey S Pitt^{1,2,3*}

¹Department of Medicine, Duke University Medical Center, Durham, United States;

²Ion Channel Research Unit, Duke University Medical Center, Durham, United States;

³Department of Neurobiology, Duke University Medical Center, Durham, United States

Abstract Rapid firing of cerebellar Purkinje neurons is facilitated in part by a voltage-gated Na⁺ (Na_v) 'resurgent' current, which allows renewed Na⁺ influx during membrane repolarization. Resurgent current results from unbinding of a blocking particle that competes with normal channel inactivation. The underlying molecular components contributing to resurgent current have not been fully identified. In this study, we show that the Na_v channel auxiliary subunit FGF14 'b' isoform, a locus for inherited spinocerebellar ataxias, controls resurgent current and repetitive firing in Purkinje neurons. FGF14 knockdown biased Na_v channels towards the inactivated state by decreasing channel availability, diminishing the 'late' Na_v current, and accelerating channel inactivation rate, thereby reducing resurgent current and repetitive spiking. Critical for these effects was both the alternatively spliced FGF14b N-terminus and direct interaction between FGF14b and the Na_v C-terminus. Together, these data suggest that the FGF14b N-terminus is a potent regulator of resurgent Na_v current in cerebellar Purkinje neurons.

DOI: [10.7554/eLife.04193.001](https://doi.org/10.7554/eLife.04193.001)

*For correspondence: geoffrey.pitt@duke.edu

Competing interests: The authors declare that no competing interests exist.


Funding: See page 13

Received: 30 July 2014

Accepted: 29 September 2014

Published: 30 September 2014

Reviewing editor: Gary L Westbrook, Vollum Institute, United States

 Copyright Yan et al. This article is distributed under the terms of the [Creative Commons Attribution License](https://creativecommons.org/licenses/by/4.0/), which permits unrestricted use and redistribution provided that the original author and source are credited.

Introduction

Cerebellar Purkinje neurons, which provide the sole output from the cerebellar cortex, display a repetitive firing behavior driven by voltage-gated Na⁺ channels (Na_v channels). Fast repetitive firing in Purkinje neurons is promoted by unusual characteristics associated with Na_v channel inactivation, whereby channels recover unusually rapidly from inactivation and in doing so pass a 'resurgent' sodium current, which helps drive the cell to fire a subsequent action potential. The molecular components underlying the peculiar properties of Na_v channels in Purkinje neurons have not been definitively identified.

Several features of Na_v currents in cerebellar Purkinje neurons, however, set them apart from Na_v currents recorded in other neurons. First, more than half of the Na_v current in Purkinje neurons is carried by Na_v1.6, an isoform for which inactivation is less complete compared to other Na_v channels (*Raman et al., 1997*). Examination of Na_v currents in cerebellar Purkinje neurons from *Scn8a*^{-/-} mice showed that, compared to the other resident Na_v channels, the *Scn8a*-encoded Na_v1.6 channels have a relatively large 'late' (non-inactivating) component and Na_v1.6 channels have increased availability (depolarized V_{1/2} for steady-state inactivation). Second, Na_v channels in cerebellar Purkinje neurons display an unusual transient re-opening during repolarization, which is identified as 'resurgent' Na_v current (*Raman and Bean, 1997*). This resurgent current derives from an unblocking of open channels by a peptide moiety that can be eliminated by the intracellular application of trypsin or chymotrypsin proteases into the cytoplasm (*Grieco et al., 2005*). The blocking particle acts only on open channels and competes with the inactivation process to prevent channels from entering an absorbed, inactivated state. During action potential repolarization, unblocking of these channels then allows Na⁺ influx that can initiate a subsequent action potential (*Khaliq et al., 2003*). Since the Na_v current in Purkinje

eLife digest The cerebellum is a region of the brain that is involved in motor control, and it contains a special type of nerve cells called Purkinje neurons. Messages travel along neurons as electrical signals carried by sodium ions, which have a positive electric charge. Normally, when a neuron is 'at rest', the plasma membrane that surrounds the neuron prevents the sodium ions outside the cell from entering. To send an electrical signal, voltage-sensitive proteins in the membrane called sodium channels open up. This allows the sodium ions to enter the cell by passing through a pore in the channel protein, thereby changing the voltage across the membrane.

Once sodium channels open, they rapidly become 'locked' in a closed state, which allows the membrane voltage to return to its original value before another signal can be sent. This locked state also prevents sodium channels from reopening quickly. As a consequence most neurons cannot send successive electrical signals rapidly. Purkinje neurons are unusual because they can send many electrical signals in quick succession—known as rapid firing—without having to be reset each time.

Rapid firing is possible in Purkinje neurons because the channel proteins can be reopened to allow more Na⁺ to enter the cell, but it is not clear how this is controlled. Now, based on experiments on Purkinje neurons isolated from mice, Yan et al. have shown that a protein called FGF14 that binds to the sodium channel proteins can help them to reopen quickly in order to allow rapid firing.

Spinocerebellar ataxia is a degenerative disease caused by damage to the cerebellum that leads to loss of physical coordination. Some patients suffering from this disease carry mutations in the gene that makes the FGF14 protein. Therefore, understanding the role of FGF14 in the rapid firing of Purkinje neurons may aid the development of new treatments for this disease.

DOI: [10.7554/eLife.04193.002](https://doi.org/10.7554/eLife.04193.002)

neurons carried by Na_v1.6 is relatively resistant to inactivation, it is particularly susceptible to open block by the peptide moiety. Why Na_v1.6 channels in cerebellar Purkinje neurons are relatively resistant to inactivation, however, is unknown.

Here, we focused on the role of the ion channel regulator FGF14, which is enriched in cerebellar granule and Purkinje neurons (Wang et al., 2002). FGF14 is one of four fibroblast growth factor homologous factors (FHF), members of the fibroblast growth factor (FGF) superfamily sharing a FGF-like core but having extended N- and C-termini not found in other FGFs. Individual FHF undergo alternative splicing that generates distinct N-termini, none of which contain a signal sequence (Smallwood et al., 1996; Munoz-Sanjuan et al., 2000). Thus, unlike other FGFs they are not secreted and do not function as growth factors (Smallwood et al., 1996). Instead, FHF remain intracellular and modulate various ion channels. FHF can bind directly to the cytoplasmic C-terminal domains (CTDs) of Na_v channels (Liu et al., 2001) and regulate Na_v channel function (Lou et al., 2005). Further, FGF14 is a potent regulator of both Na_v1.1 and Na_v1.6 (Lou et al., 2005; Laezza et al., 2009), the two dominant Na_v channels in cerebellar Purkinje neurons (Raman et al., 1997; Kalume et al., 2007). FHF also regulate voltage-gated Ca²⁺ channels through a mechanism that does not appear to involve a direct interaction (Hennessey et al., 2013; Yan et al., 2013). An ataxia phenotype in *Fgf14*^{-/-} mice highlights the role of FGF14 in cerebellar physiology and the development of spinocerebellar ataxia type 27 (SCA27) in patients with either FGF14 haploinsufficiency or a dominant negative *FGF14* mutation (Wang et al., 2002; van Swieten et al., 2003; Dalski et al., 2005) underscores the role of FGF14 in disease.

Using shRNA knockdown of endogenous FGF14 in cultured cerebellar Purkinje neurons and replacement with informative mutants that blocked binding of FGF14 to Na_v CTDs and eliminated the FGF14 extended N-terminus, we found that FGF14, and especially the N-terminus of the FGF14b isoform exerts specific kinetic effects on cerebellar Na_v channels that support repetitive firing and therefore provides new information on the pathophysiology of SCA27.

Results

To test whether FGF14 was a contributor to regulation of Na_v current in cerebellar Purkinje neurons, we first confirmed its expression in cerebellum and demonstrated that FGF14 co-immunoprecipitates with Na_v1.6 channels in mouse cerebellar lysates (Figure 1A). Although FGF14 was previously shown

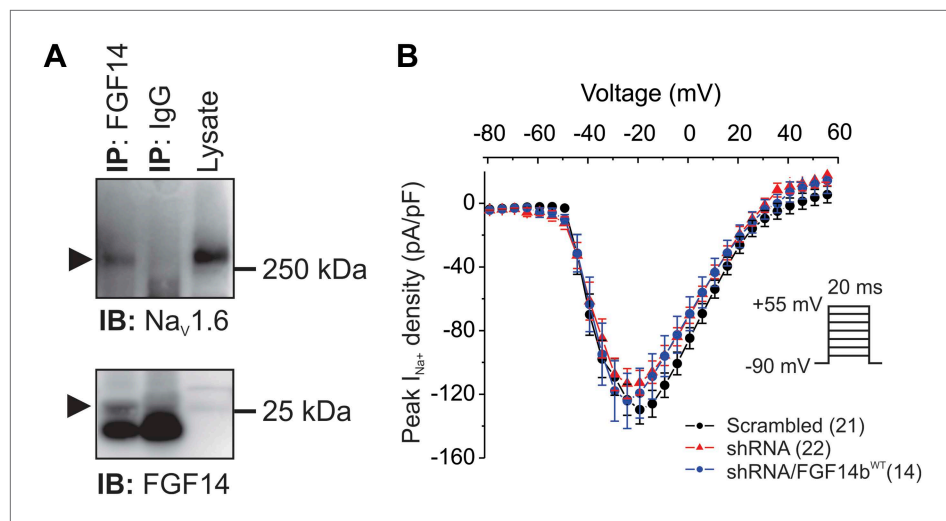


Figure 1. FGF14 is a component of the $Na_v1.6$ macromolecular complex in mouse cerebellum, but shRNA knockdown does not affect Na_v current density in cultured cerebellar Purkinje neurons. **(A)** Co-immunoprecipitation (IP) of $Na_v1.6$ by FGF14 from mouse cerebellum and immunoblot (IB) with the indicated antibodies. M_w markers are indicated on right. Arrowheads indicate $Na_v1.6$ (top panel) and FGF14 (bottom panel). Intense signal in bottom panel below the FGF14 signal is immunoglobulin light chain. **(B)** Current–voltage relationships (normalized to cell capacitance) of transient Na_v currents from cerebellar Purkinje neurons transfected with Scrambled control shRNA (Scrambled), FGF14 shRNA (shRNA), or FGF14 shRNA plus the shRNA-resistant FGF14b^{WT} (shRNA/FGF14b^{WT}). The number of neurons tested, N , is in parentheses. Inset shows schematic of voltage protocol.

DOI: [10.7554/eLife.04193.003](https://doi.org/10.7554/eLife.04193.003)

to co-immunoprecipitate with $Na_v1.6$ in a heterologous expression system (Laezza *et al.*, 2009), co-immunoprecipitation between FGF14 and $Na_v1.6$ channels has not been reported from brain.

To evaluate the consequences of FGF14 haploinsufficiency in SCA27, we used a previously validated shRNA (Yan *et al.*, 2013) to knockdown endogenous FGF14 in cultured cerebellar Purkinje neurons. Knockdown of FGF14 did not affect Na_v current density compared to the Na_v current density recorded in neurons transfected with a control shRNA (Figure 1B). Because knockout of *Fgf14* reduced spiking activity (Goldfarb *et al.*, 2007) but Na_v current density was unaffected in *Fgf14* knockout or knockdown, we hypothesized that the absence of FGF14 must affect Na_v kinetic properties in ways that prevent repetitive firing. We therefore examined Na_v kinetic properties in more detail.

Voltage dependence of activation was unaffected by FGF14 knockdown (Figure 2A), but the $V_{1/2}$ of steady-state inactivation was shifted about -10 mV, thereby decreasing channel availability (Figure 2B and Table 1). When we co-expressed a FGF14b cDNA with synonymous substitutions rendering it resistant to the FGF14 shRNA (FGF14b^{WT}), the $V_{1/2}$ of steady-state inactivation was restored to the control voltage; activation was unaffected (Figure 2A–B and Table 1). The ‘rescue’ of steady-state inactivation by expression of the shRNA-insensitive FGF14 provided additional demonstration of the specificity of our shRNA targeting strategy (and see similar rescue for additional parameters below). In addition to the decreased channel availability, we observed that FGF14 knockdown accelerated inactivation kinetics (Figure 2C–D). FGF14 knockdown also reduced the late Na_v current (Figure 2E–F). Thus, by several different kinetic measures, FGF14 knockdown in cerebellar Purkinje neurons biased the endogenous Na_v channels towards entering the inactivated state. We anticipated, therefore, that FGF14 knockdown should reduce Na_v resurgent current amplitude, a key feature that allows cerebellar Purkinje neurons to fire repetitively. Indeed, the amplitude of the resurgent Na_v current (Figure 2G–J) was markedly diminished using a well-established protocol to elicit Na_v resurgent current (Raman and Bean, 1997). As with the other kinetic properties of Na_v currents (above), co-expression of FGF14b^{WT} in the presence of the shRNA provided a complete rescue (Figure 2G–J). While FGF14 knockdown reduced the amplitude of resurgent Na_v current, it did not significantly affect the time to peak (Figure 2K).

To determine how FGF14 regulates Na_v kinetics and Na_v resurgent current, we turned our focus to the FGF14 N-terminus. The alternatively spliced N-termini of various FHF s have been shown to exert

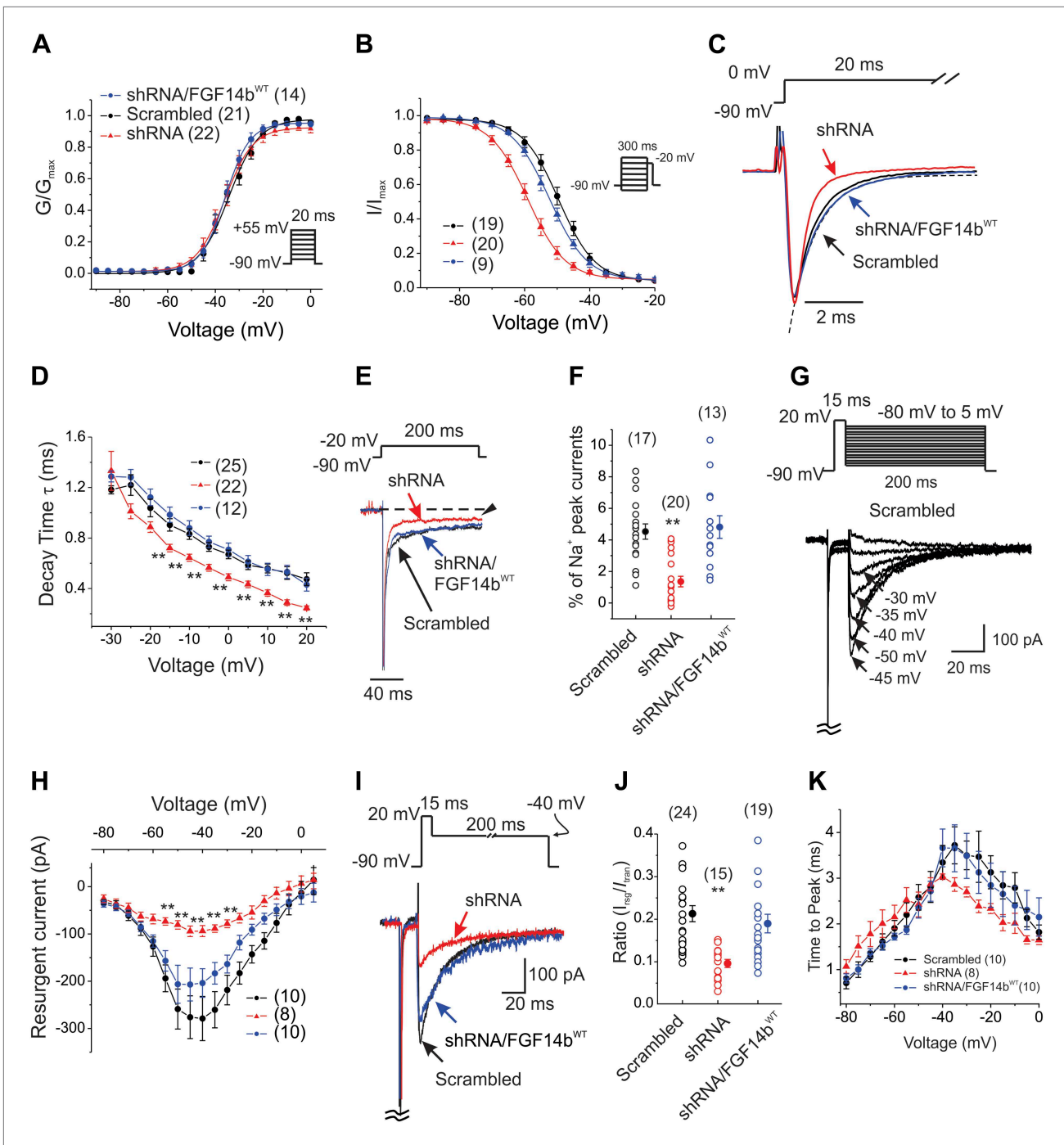


Figure 2. FGF14 knockdown in cerebellar Purkinje neurons affects multiple Na_v channel biophysical properties. **(A and B)** Voltage-dependence of Na_v channel activation and steady-state inactivation in cerebellar Purkinje neurons transfected with Scrambled control shRNA (Scrambled), FGF14 shRNA (shRNA), or FGF14 shRNA plus the shRNA-resistant FGF14b^{WT} (shRNA/FGF14^{WT}). The number of neurons tested, *N*, is in parentheses. Inset shows schematic of voltage protocol. **(C)** Exemplar normalized Na_v current traces elicited with a step depolarization to 0 mV from a holding potential of -90 mV and an exemplar single exponential fit (for Scrambled) for the time constant (τ) of inactivation (dotted line). **(D)** τ of inactivation at the indicated test voltages. The number of neurons tested, *N*, is in parentheses. ****p** < 0.01. **(E)** Exemplar normalized TTX-sensitive late Na_v currents at -20 mV (measured at 150 ms, arrowhead) from a holding potential of -90 mV. **(F)** Amplitude of late Na_v current as a % of peak (transient) Na_v current. The number of neurons tested, *N*, is in parentheses. ****p** < 0.01. **(G)** Voltage-clamp protocol and exemplar TTX-sensitive resurgent Na_v currents recorded from cerebellar Purkinje neurons transfected with Scrambled control shRNA. The transient current has been clipped. **(H)** Current-voltage relationship of Na_v resurgent currents. The number of neurons tested, *N*, is in parentheses. ****p** < 0.01. **(I)** Overlay of Na_v resurgent currents for the indicated conditions recorded with Figure 2. *Continued on next page*

Figure 2. Continued

the indicated voltage protocol. The transient current has been clipped. (J) Ratio of peak Na_v resurgent current (at +20 mV) to transient Na_v current (at -10 mV). The number of neurons tested, N , is in parentheses. $**p < 0.01$. (K) Time to peak of Na_v resurgent current over a broad range of voltages. The number of neurons tested, N , is in parentheses. $**p < 0.01$.

DOI: 10.7554/eLife.04193.004

specific effects on Na_v currents (Lou et al., 2005; Rush et al., 2006), including the regulation of inactivation kinetics (Laezza et al., 2009; Dover et al., 2010), but the role of the FGF14 N-termini have not been investigated in cerebellar Purkinje neurons. FGF14b is the predominant FGF14 splice variant expressed in brain (Wang et al., 2000, 2011) and the FGF14 splice variant found in the cytoplasm; FGF14a is localized to the nucleus (Wang et al., 2000). To test the specific roles of the FGF14b N-terminus, we expressed a FGF14 in which the N-terminus was deleted (FGF14 Δ^{NT}). Because the interaction site for the Na_v CTD on FHF lies within the conserved core domain (Wang et al., 2012), deletion of the N-terminus does not affect interaction with the Na_v CTD. Thus, the FGF14 Δ^{NT} exerts a dominant negative effect by competing with endogenous FGF14 for interaction with the Na_v CTD (Figure 3A). Current density (Figure 3B) and the $V_{1/2}$ of activation (Figure 3C and Table 1) were unaffected. However, expression of FGF14 Δ^{NT} shifted the $V_{1/2}$ of steady-state inactivation about -10 mV (Figure 3C), accelerated kinetics of inactivation (Figure 3D), reduced the late Na_v current (Figure 3E), and diminished resurgent current (Figure 3F) to a degree similar to or even greater than shRNA knockdown. FGF14 Δ^{NT} diminished resurgent Na_v current even more effectively than shRNA knockdown of FGF14. As a control, we overexpressed the FGF14b $^{\text{WT}}$ that had rescued the parameters affected by shRNA knockdown (Figure 1). Overexpression of FGF14b $^{\text{WT}}$ here was without effect (Figure 3 and Table 1). Not only did this serve as a control for FGF14 Δ^{NT} , but these data suggest that endogenous FGF14b is saturating. These data also suggest that FGF14b's main regulatory component for Purkinje neuron Na_v currents lies within the FGF14b N-terminus.

The dominant negative effect exerted by FGF14 Δ^{NT} as it replaced the endogenous FGF14 on the Na_v CTD implied that although FGF14 regulates Na_v current through its N-terminus, it may require that FGF14 be in direct interaction with the channel. To test this hypothesis specifically, we designed a FGF14b that was unable to bind to the channel CTD and examined whether expression of this mutant could restore the diminished resurgent current resulting from shRNA knockdown of FGF14. Structural determination of a ternary complex containing FGF13, the $\text{Na}_v1.5$ CTD, and calmodulin had identified key amino acids on the conserved FHF interaction surface that participated in the interaction with the conserved Na_v CTD surface (Wang et al., 2012). We focused on a highly conserved Arg in the FHF core domain (Arg57 in FGF13U, equivalent to Arg117 in FGF14b), which inserts into a deep pocket on the $\text{Na}_v1.5$ CTD binding surface (Figure 4A). We therefore generated the homologous R117A mutant (FGF14b $^{\text{R/A}}$) in the FGF14b shRNA-resistant cDNA background and tested whether FGF14b $^{\text{R/A}}$ could bind to the intact $\text{Na}_v1.6$. Although immunoprecipitation of FGF14b $^{\text{WT}}$ from lysates of HEK293 cells transfected with FGF14b $^{\text{WT}}$ and $\text{Na}_v1.6$ showed co-immunoprecipitation of $\text{Na}_v1.6$, the mutant FGF14b $^{\text{R/A}}$ was unable to co-immunoprecipitate $\text{Na}_v1.6$ (Figure 4B). Thus, mutation of R117A in FGF14b prevents interaction with $\text{Na}_v1.6$. We therefore transfected the shRNA-resistant FGF14b $^{\text{R/A}}$ (or the shRNA-resistant FGF14b $^{\text{WT}}$) along with the FGF14 shRNA into cultured cerebellar Purkinje neurons to determine the effect of FGF14 interaction with $\text{Na}_v1.6$ on Na_v currents. Expression of FGF14b $^{\text{R/A}}$ after shRNA knockdown of endogenous FGF14 had no effect on Na_v current density (Figure 4C). In contrast to the rescue afforded by FGF14b $^{\text{WT}}$, FGF14b $^{\text{R/A}}$ did not rescue the key parameters that lead to increased inactivation observed after FGF14 shRNA. Na_v late current and the time constant of inactivation were not different from shRNA (Figure 4D–F). Consistent with these findings, we observed the expected reduction in resurgent Na_v current (Figure 4G–H). Thus, the FGF14 N-terminus must exert its key effects through FGF14's direct interaction with the Na_v C-terminus.

Because the absence of the FGF14 or its N-terminus accelerated Na_v channel inactivation, diminished late current, and decreased resurgent current, we anticipated that the resultant bias towards Na_v inactivation would adversely affect excitability in cerebellar Purkinje neurons. We tested this hypothesis by determining the effects of the FGF14 and its N-terminus on action potential threshold and on the number of action potentials evoked with depolarizing current injections in current-clamp mode. Under our culture conditions (≤ 14 days in vitro), we found that 8–10% of cerebellar Purkinje

Table 1. Na_v current activation and inactivation parameters in cerebellar Purkinje neurons

	Activation			Inactivation		
	V _{1/2} (mV)	K	n	V _{1/2} (mV)	K	n
Scrambled	-34.4 ± 1.5	4.0 ± 0.3	21	-49.7 ± 1.2	4.2 ± 0.1	19
shRNA	-35.0 ± 1.9	4.3 ± 0.5	22	-59.0 ± 1.2**	4.7 ± 0.2	20
shRNA/FGF14b ^{WT}	-35.5 ± 1.5	3.9 ± 0.3	14	-52.0 ± 0.9	5.2 ± 0.3	9
shRNA/FGF14 ^{RA}	-33.2 ± 1.5	3.5 ± 0.2	12	-50.9 ± 1.4	4.4 ± 0.3	11
FGF14b ^{WT}	-33.1 ± 1.4	4.5 ± 0.5	14	-50.6 ± 1.3	4.9 ± 0.3	10
FGF14Δ ^{NT}	-33.9 ± 2.0	3.9 ± 0.5	14	-59.1 ± 0.8**	4.7 ± 0.3	15

Mean ± s.e.m. (n), **p < 0.01 compared to Scrambled control.

DOI: [10.7554/eLife.04193.005](https://doi.org/10.7554/eLife.04193.005)

neurons exhibit spontaneous action potentials (firing rate 5–20 Hz) with regular and irregular patterns. When neurons were cultured for extended periods (>20 days in vitro), we observed that ~50% of Purkinje neurons spontaneously fired—more similar to acutely isolated Purkinje neurons (Raman and Bean, 1999) and cultured Purkinje neurons (Grul and Franklin, 1987). These data suggest that spontaneous activity depends upon the maturity of the neurons in culture. Because of the difficulty in achieving voltage clamp on Purkinje neurons ≥14 days in vitro, our voltage-clamp experiments were performed on the younger cells (Figures 2–4). Thus, we continued with immature neurons for these experiments, and focused on measuring evoked action potentials rather than spontaneous action potentials. Single action potentials were evoked by a 10-ms current injection with 5-pA increments to determine the current threshold to initiate an action potential. Figure 5A–B and Table 2 show that FGF14 knockdown and expression of the dominant negative FGF14bΔ^{NT} markedly increased the current threshold to produce an action potential; other action potential parameters were not affected. Rescue of FGF14 knockdown by co-expression of FGF14b^{WT} restored the current threshold to control levels. Rescue with the non-interacting FGF14b^{RA} did not. We also analyzed the number of actions evoked during 600 ms current injection over a wide range of current amplitudes. The number of action potentials evoked was significantly larger in control (scrambled shRNA) neurons than in neurons transfected with FGF14 shRNA. Rescue with FGF14b^{WT}, but not FGF14b^{RA}, restored the number of evoked action potentials to control levels. Expression of the dominant negative FGF14bΔ^{NT} reduced the number of evoked action potentials to the level observed after FGF14 knockdown (Figure 5C–D). Thus, as observed for the individual Na_v channel kinetic parameters, FGF14b, and its N-terminus specifically, is a critical regulator of neuronal firing and intrinsic membrane properties.

Discussion

Although FGF14 haploinsufficiency is associated with spinocerebellar ataxia (Dalski et al., 2005) and intrinsic excitability of cerebellar Purkinje neurons is reduced in *Fgf14*^{-/-} mice (Shakkottai et al., 2009), the detailed multifactorial molecular mechanisms by which FGF14 affects neuronal excitability were not previously known. We had found that FGF14 knockdown in cerebellar granule neurons reduced presynaptic voltage-gated Ca²⁺ currents and thereby affected neurotransmission at the cerebellar granule neuron to Purkinje neuron synapse (Yan et al., 2013). Here, we found that FGF14b in cerebellar Purkinje neurons affects multiple kinetic parameters of Na_v channels, thereby reducing the resurgent Na_v current that underlies repetitive firing. Together, the accelerated inactivation, reduced channel availability, and decreased late current observed after FGF14 knockdown bias Na_v channels to the inactivated state. Thus, the blocking particle that competes with the inactivation gate for open Na_v channels is disadvantaged. Consequently, the resurgent current, and the resulting ability to support repetitive firing in Purkinje neurons, is reduced as we observed. Thus, our data show that an essential regulatory feature of FGF14 in cerebellar Purkinje neurons is to slow Na_v channel inactivation in order to foster resurgent current.

Resurgent current results from the actions on Na_v1.6 of a putative blocking particle, which is thought to be the cytoplasmic C-terminal peptide of the Na_v auxiliary Na_vβ4 subunit (Grieco et al., 2005).

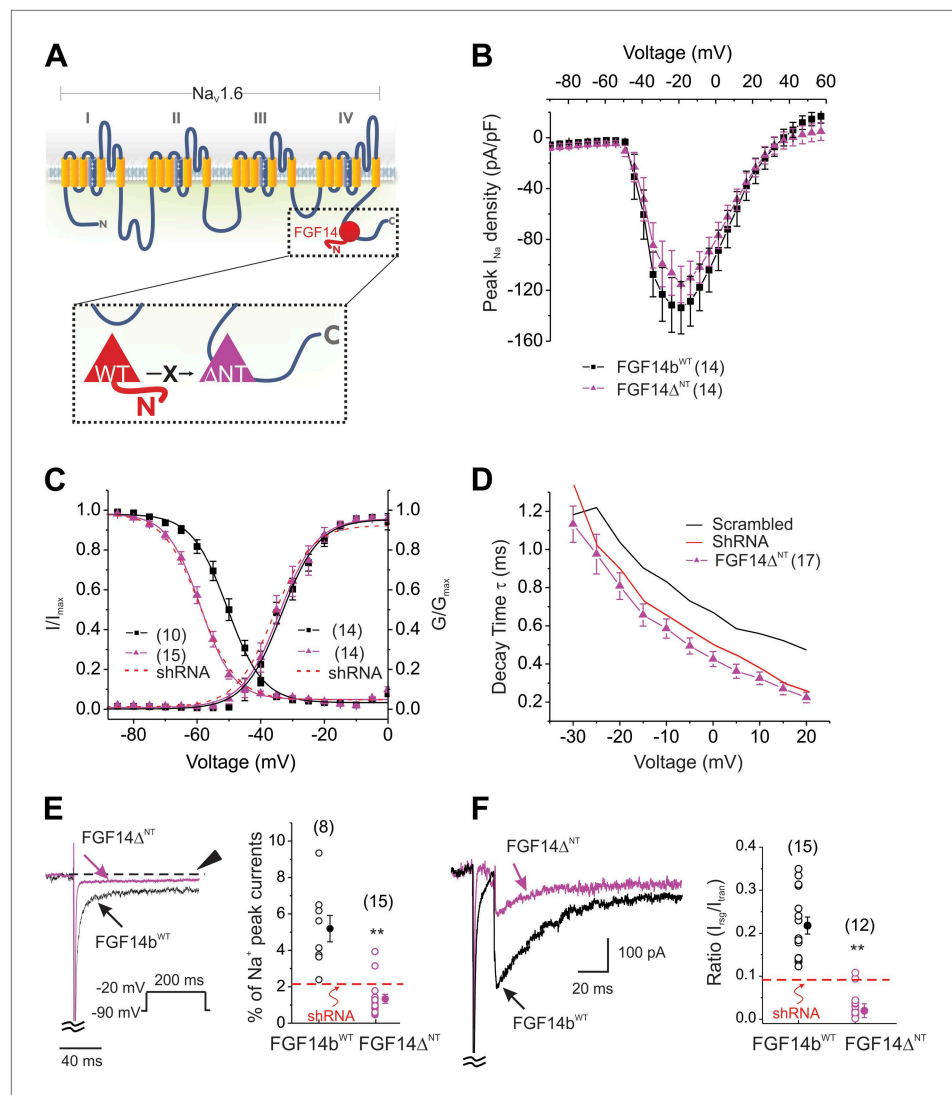


Figure 3. Expression of the dominant negative FGF14 Δ ^{NT} affects multiple Na_v channel biophysical properties indicating essential roles for the FGF14 N-terminus. **(A)** Schematic of endogenous wild type (WT) FGF14 binding to the C-terminus of the Na_v1.6 α subunit (top) and magnified schematic of the expressed FGF14 Δ ^{NT} preventing binding of the WT FGF14 (in box). **(B)** Current–voltage relationships (normalized to cell capacitance) of transient Na_v currents from cerebellar Purkinje neurons transfected with FGF14b^{WT} or FGF14 Δ ^{NT}. The number of neurons tested, *N*, is in parentheses. The current–voltage relationship for Scrambled control shRNA (from **Figure 1**) is shown for comparison. **(C)** Voltage dependence of Na_v channel activation and steady-state inactivation in cerebellar Purkinje neurons transfected with FGF14b^{WT} or FGF14 Δ ^{NT}. The number of neurons tested, *N*, is in parentheses. The curves for Scrambled control shRNA (from **Figure 1**) are shown for comparison. **(D)** τ of inactivation at the indicated test voltages. The number of neurons tested, *N*, is in parentheses. **(E)** Exemplar normalized TTX-sensitive late Na_v currents at –20 mV (measured at 150 ms, arrowhead) from a holding potential of –90 mV. The number of neurons tested, *N*, is in parentheses. **(F)** Overlay of Na_v resurgent currents recorded from cerebellar Purkinje neurons transfected with FGF14 Δ ^{NT} or FGF14b^{WT} and ratio of peak Na_v resurgent current (at +20 mV) to transient Na_v current (at –10 mV). The number of neurons tested, *N*, is in parentheses. The average for FGF14 shRNA knockdown (**Figure 1**) is shown for comparison. *******p* < 0.01.

DOI: 10.7554/eLife.04193.006

Nevertheless, the actions of Na_v β 4 are not sufficient to generate resurgent Na_v current (**Chen et al., 2008; Aman et al., 2009**), suggesting that other components of the Na_v channel complex may be necessary for proper regulation of resurgent Na_v current in cerebellar Purkinje neurons. Here, our knockdown experiments and expression of the dominant negative FGF14b Δ ^{NT} show that FGF14b, and

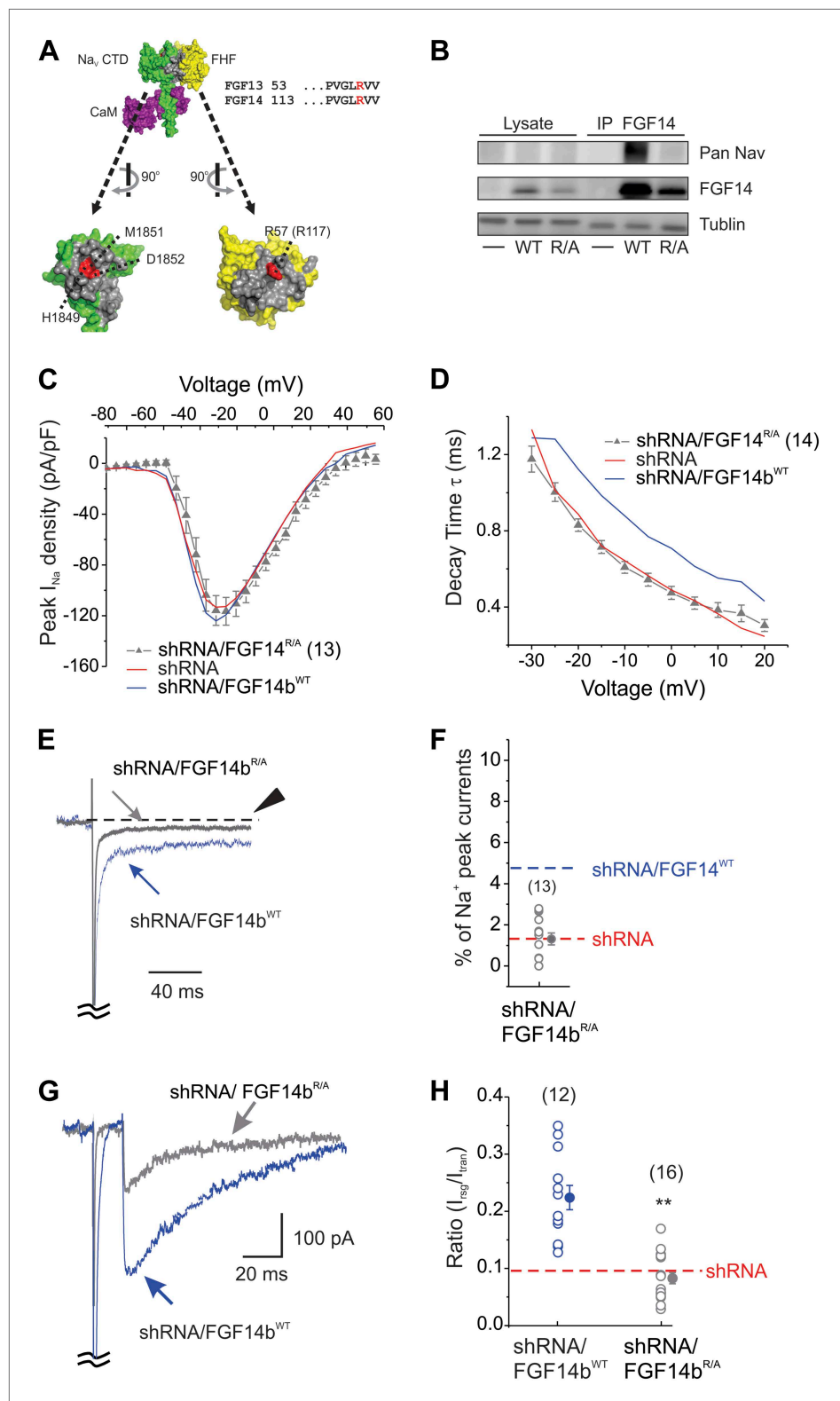


Figure 4. The FGF14b^{R/A} mutant that prevents interaction with the Na_v C-terminus cannot rescue Na_v kinetic effects of FGF14 knockdown. **(A)** Surface representation of the crystal structure of a ternary complex containing the Na_v1.5 C-terminus domain (CTD, green), FGF13 (yellow), and calmodulin (purple); the interaction surfaces are colored gray (PDB ID: 4DCK). The critical R57 in FGF13 (equivalent to R117 in FGF14) is indicated in red, as is its binding pocket *Figure 4. Continued on next page*

Figure 4. Continued

on the Na_v1.5 CTD. **(B)** Co-immunoprecipitation (IP) of Na_v1.6 and FGF14b^{WT} or FGF14b^{R/A} expressed in HEK293 cells, showing that the FGF14b^{R/A} is unable to interact with the intact Na_v1.6. Immunoblots (IB) were performed with the indicated antibodies. **(C)** Current–voltage relationship (normalized to cell capacitance) of transient Na_v currents from cerebellar Purkinje neurons transfected with FGF14b^{R/A}. The number of neurons tested, *N*, is in parentheses. The current–voltage relationship for FGF14 knockdown (shRNA) and knockdown rescued with shRNA-insensitive FGF14b^{WT} (shRNA/FGF14b^{WT}) from **Figure 1** are shown for comparison. **(D)** τ of inactivation at the indicated test voltages. The number of neurons tested, *N*, is in parentheses. **(E)** Exemplar normalized TTX-sensitive late Na_v currents at –20 mV (measured at 150 ms, arrowhead) from a holding potential of –90 mV and **(F)** amplitude of late Na_v current as a % of peak (transient) Na_v current. The number of neurons tested, *N*, is in parentheses. Averages for shRNA and for shRNA/FGF14b^{WT} (see **Figure 1**) are shown for comparison. **(G)** Overlay of Na_v resurgent currents recorded from cerebellar Purkinje neurons transfected with FGF14b^{R/A} or FGF14b^{WT} and **(H)** ratio of peak Na_v resurgent current (at +20 mV) to transient Na_v current (at –10 mV). The number of neurons tested, *N*, is in parentheses. The average for FGF14 shRNA knockdown (**Figure 1**) is shown for comparison. ***p* < 0.01.

DOI: [10.7554/eLife.04193.007](https://doi.org/10.7554/eLife.04193.007)

specifically its N-terminus, strongly influence resurgent Na_v current. FGF14 knockdown caused a ~60% reduction. Expression of FGF14 Δ ^{NT} was even more efficient, resulting in a ~85% reduction, perhaps because overexpression of FGF14 Δ ^{NT} was more efficient in replacing endogenous FGF14b than shRNA knockdown was in eliminating endogenous FGF14b. Thus, FGF14 may cooperate with Na_v β 4 to generate resurgent current, perhaps by biasing Na_v1.6 channels towards inactivation and thereby disadvantaging the blocking particle. Our results examining effects on total Na_v current must be assessed in the context of FGF14 effects not only on Na_v1.6 channels but also on Na_v1.1 channel, the other major source of Na_v currents in cerebellar Purkinje neurons (Kalume et al., 2007). Those Na_v channels are also influenced by FGF14 (Lou et al., 2005). Thus, the effects on resurgent current that we attribute to FGF14 may result from FGF14's overall influence of Na_v channel kinetics within Purkinje neurons.

Our results may also provide some insight into the more variable phenotypes and decreased penetrance in spinocerebellar ataxia patients with FGF14 haploinsufficiency (Dalski et al., 2005; Coebergh et al., 2013) vs patients with a FGF14 mutation (FGF14b^{F1505}) found in a large Dutch spinocerebellar ataxia kindred (van Swieten et al., 2003). Studies in hippocampal neurons suggest that the FGF14b^{F1505} mutant exerts a dominant negative mechanism in which the axon initial segment is depleted of Na_v channels and Na_v current density is reduced (Laezza et al., 2007). Here, we found no effect on Na_v current density in cerebellar Purkinje neurons after FGF14 knockdown. A reduction in Na_v current density (with the FGF14b^{F1505} mutation) compared to an effect solely on Na_v channel kinetics (with FGF14 haploinsufficiency) may explain the higher penetrance and decreased phenotypic variability in patients with the FGF14b^{F1505} mutation.

An important aspect of this study examining effects on Na_v channel kinetics was that our analyses were performed in Purkinje neurons. Studying FHF in their native cellular context appears to be crucial for defining their specific roles. Previous investigations of FGF14-dependent regulation of neuronal Na_v channels in heterologous expression systems led to different conclusions from experiments in neurons. For example, expression of Na_v1.6 and FGF14b^{WT} in ND7/23 cells almost eliminated Na_v current density (Laezza et al., 2009) while overexpression of FGF14b^{WT} in hippocampal neurons increased Na_v current density (Laezza et al., 2007). Similarly, expression of FGF14 Δ ^{NT} in ND7/23 cells increased current density, while here we observed that FGF14 Δ ^{NT} expression in cerebellar Purkinje neurons exerted dominant-negative effects upon Na_v channel kinetics, but no consequences for Na_v current density. While the etiology of the different results in neurons compared to heterologous expression systems is not known, we speculate that additional regulatory factors present in neurons are necessary for physiologic regulation of Na_v channels by FHFs. Indeed, we have observed similarly disparate results for the related FGF13 and the cardiac Na_v1.5 channel. In HEK293 cells, FGF13 co-expression reduces Na_v1.5 current density (not shown), but we showed that the role FGF13 in cardiomyocytes is to increase Na_v current density (Wang et al., 2011; Hennessey et al., 2013).

Finally, our data also provide information about possible consequences of FGF14 overexpression, hypothesized as pathologic in rare cases. Some patients with spinocerebellar ataxia, but not controls, harbor synonymous variants in FGF14. These variants encode a more frequently used codon than the

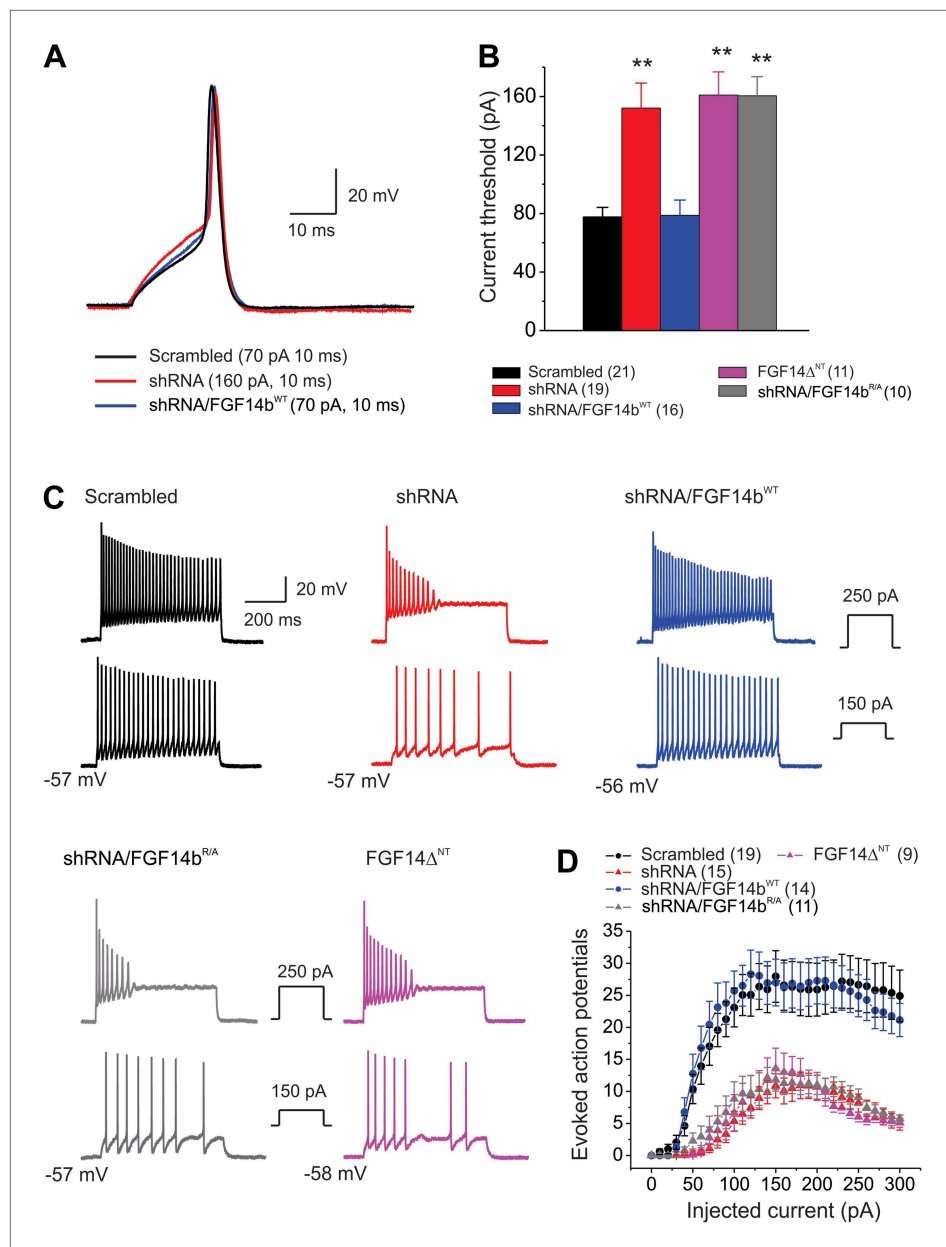


Figure 5. Action potential dynamics and repetitive spiking are dependent upon FGF14 and its N-terminus. (A) Overlay of single action potentials evoked with a 10 ms current injection (current amplitude shown in parentheses). (B) Current threshold to induce action potentials for the indicated conditions. $^{**}p < 0.01$. The number of neurons tested, N , is in parentheses. Additional summary data are presented in **Table 2**. (C) Example evoked action potentials for the indicated treatments at two separate current injection amplitudes (shown in insets). The resting membrane potential is indicated. (D) The number of evoked action potentials for the indicated amplitude of current injection. The number of neurons tested, N , is in parentheses.
 DOI: [10.7554/eLife.04193.008](https://doi.org/10.7554/eLife.04193.008)

wild type sequence, leading to the hypothesis that patients with these variants would overexpress *FGF14* as a cause of disease (Dalski et al., 2005). We found, however, that overexpression of *FGF14b*^{WT} did not affect current density or any of the measured Na_v kinetic properties (Figure 3 and Table 1). Thus, if these variants identified in spinocerebellar ataxia patients are truly associated with disease, our data suggest mechanisms other than *FGF14* overexpression.

In summary, these data add to a growing appreciation of physiologic and pathophysiologic roles for FGFs in neurons. In the case of spinocerebellar ataxia, our data suggest that *FGF14* is a critical

Table 2. Intrinsic membrane properties and single action potential (AP) characteristics measured in cerebellar Purkinje neurons

	Scrambled	shRNA	shRNA/FGF14b ^{WT}	shRNA/FGF14b ^{RA}	FGF14 ^{ΔNT}
Input resistance (MΩ)	221.8 ± 15.8 (7)	238.0 ± 49.5 (11)	266.6 ± 24.5 (11)	225.9 ± 10.8 (6)	269.5 ± 30.2 (6)
Resting membrane potential (mV)	-54.5 ± 1.3 (21)	-55.8 ± 1.2 (19)	-54.4 ± 1.0 (16)	-55.4 ± 0.7 (10)	-54.9 ± 1.4 (11)
Current threshold (pA)	77.8 ± 6.4 (21)	142.1 ± 18.5 (19)**	78.8 ± 10.4 (16)	170.5 ± 16.7 (10)**	191.0 ± 22.1 (11)**
AP threshold (mV)	-35.6 ± 1.0 (21)	-32.8 ± 1.2 (19)	-34.5 ± 0.8 (16)	-32.8 ± 1.4 (10)	-32.7 ± 0.8 (11)
AP amplitude (mV)	78.8 ± 3.2 (21)	77.5 ± 2.8 (19)	78.9 ± 4.5 (16)	79.1 ± 4.3 (10)	73.1 ± 4.7 (11)
AP duration (ms)	2.3 ± 0.2 (21)	2.0 ± 0.1 (19)	2.2 ± 0.1 (16)	1.8 ± 0.1 (10)	2.1 ± 0.3 (11)

Mean ± s.e.m. (n), **p < 0.01 compared to Scrambled control.

DOI: [10.7554/eLife.04193.009](https://doi.org/10.7554/eLife.04193.009)

regulator of the ability of cerebellar Purkinje neuron Na_v channels to support resurgent Na_v current and thereby allow Purkinje neurons to fire repetitively. Thus, we provide a molecular understanding for the observation that FGF14 regulates Purkinje neuron intrinsic excitability (*Shakkottai et al., 2009*). In combination with our data showing that FGF14 also regulates presynaptic voltage-gated Ca²⁺ channels at the cerebellar granule cell to Purkinje cell synapse, these data pinpoint several specific mechanisms by which mutations in *FGF14* underlie spinocerebellar ataxia.

Materials and methods

Primary cerebellar neuron culture and transfection

This study was performed in strict accordance with the recommendations in the Guide for the Care and Use of Laboratory Animals of the National Institutes of Health. All of the animals were handled according to approved Institutional Animal Care and Use Committee (IACUC) of Duke University (protocol #A292-13-11). Primary dissociated cerebellar neurons were cultured as previously described (*Yan et al., 2013*) with some modifications. Briefly, primary cultures were prepared from P6-P8 C57BL6 mice. Cerebella were excised, dissected on ice, digested with 0.25% trypsin for 10 min at 37°C with Dulbecco's Modified Eagle's Medium (DMEM, Sigma, St. Louis, MO), and dissociated into single cells by gentle trituration. The cells were seeded onto coverslips coated with 50 μg/ml poly-D-lysine (Sigma) and 25 μg/ml laminin (Sigma) at a density of 2.5–3.0 × 10⁵ cells/coverslip in DMEM supplemented with 10% heat-inactivated fetal bovine serum (FBS). The neurons were maintained in a humidified incubator in 5% CO₂ at 37°C. After 15–16 hr, the medium was replaced with Basal Medium Eagle (BME, Sigma) supplemented with 2% B27 (Invitrogen), 5% FBS, 25 μM uridine, 70 μM 5-fluorodeoxyuridine, and 20 mM KCl. Neurons were transiently transfected at 4 days in vitro with 1 μg plasmid DNA and/or shRNA plasmids per coverslip with calcium phosphate. Experiments were performed 8–10 days after transfection (12–14 days in vitro). To achieve good voltage control, all recordings were performed in neurons cultured no longer than 14 days in vitro.

shRNA and cDNA construction

shRNAs targeted to FGF14 were designed with Invitrogen's RNAi Designer as previously described (*Yan et al., 2013*) and the sequences were cloned into pLVTHM (Addgene). After evaluating several candidates, we found that the most effective shRNA sequence was 5' CGCGTGGA GGCAAACCAAGTCAACAAGTGCATTCAAGAGATGCACTTGTTGACTGGTTTTGC CTCCTTTTTTAT 3', which was used for the experiments described here. The scrambled shRNA which bears no homology to genes in the rodent genome (*Wang et al., 2011*) has the sequence: 5'-CGCGTGACCC TTAGTTTATACCTATTCAAGAGATAGGTATAAACTAAGGGTCTTTTTTAT-3'. FGF14 rescue and overexpression experiments were performed with FGF14 constructs (either full-length or with the N-terminus truncated) cloned into pcDNA3.1 also containing tdTomato. Mutagenesis to obtain FGF14b^{RA} was performed using QuikChange (Agilent). All plasmids were verified by sequencing.

Electrophysiological recordings

Purkinje neurons were identified by their characteristic teardrop morphology and large size. Whole-cell Na_v currents and membrane voltage were recorded at 23–25°C using an EPC 10 USB patch

amplifier (HEKA Elektronik). The signal was filtered at 2.9 Hz and digitized at 20 Hz. Na_v currents were recorded with an extracellular solution containing (in mM) 124 NaCl, 20 TEA-Cl (tetraethylammonium Chloride), 5 HEPES (4-(2-hydroxyethyl)-1-piperazineethanesulfonic acid), 10 glucose, 0.3 CdCl_2 , 2 BaCl_2 , and 4-AP (4-aminopyridine). NaOH was added to achieve pH 7.3 (300–310 mOsm). Borosilicate glass patch pipettes (resistances within 3–4 M Ω) were filled with the following internal solution (in mM): 125 CsF, 10 NaCl, 10 HEPES, 15 TEA-Cl, 1.1 ethylene glycol tetraacetic acid (EGTA), and 0.5 Na-guanosine-5'-triphosphate (Na-GTP), pH adjusted to 7.3 with CsOH (290–300 mOsm). Tetrodotoxin (TTX)-sensitive Na_v currents were isolated by subtraction of recordings performed in 1 μM TTX from the control recordings. Series resistance was compensated >70%. Current-clamp recordings were performed after obtaining seal resistances >1.2 G Ω . The internal solution was (in mM) 130 K-gluconate, 5 NaCl, 2 MgCl_2 , 10 HEPES, 4 Mg-ATP, 0.5 Na-GTP, 0.2 EGTA, and 10 phosphocreatine. KOH was used to obtain pH 7.3 (290–300 mOsm). The external solution was (in mM) 140 NaCl, 5 KCl, 2 CaCl_2 , 1 MgCl_2 , 5 HEPES, and 10 glucose, pH adjusted to 7.3 with NaOH. Resting membrane potential was directly measured in current-clamp mode after membrane rupture and only cells with a resting membrane potential more negative than –50 mV were studied. The liquid junction potential was not corrected. Input resistance was determined from membrane voltage deflection, evoked by 600-ms hyperpolarizing current injections (0 to –300 pA in steps of 50 pA) and calculated from the measured slope. Single action potentials were elicited by 10 ms depolarizing current injections with 5-pA increments. All drugs were from Sigma Aldrich, except for TTX (Abcam Biochemicals).

Protocols and data analysis

Data analysis was performed using FitMaster (HEKA), Excel (Microsoft), and Origin software. All averaged data are presented as mean \pm SEM. Statistical significance was determined using Student's *t* or one-way ANOVA tests. Calculated *p* values of ≤ 0.05 were accepted as evidence of statistically significant differences. For current amplitude, neurons were held at –90 mV and transient Na_v current was elicited by depolarizing pulses of 20 ms from –90 mV to +55 mV in 5-mV increments. Current density was obtained by normalizing peak Na_v current to membrane capacitance. Resurgent Na_v current was evoked with repolarizing steps from +20 mV to a range of voltages between –80 mV and +5 mV in 5-mV increments for a 200-ms test pulse after 15 ms conditioning steps. Na_v activation curves were obtained by transforming current data to conductance (*G*), with the equation $G = I_{\text{Na}} / (E_m - E_{\text{rev}})$, where: I_{Na} is the peak current; E_m is the membrane potential; and E_{rev} is the reversal potential of I_{Na} ; and fitted with a Boltzmann equation of the form: $G = G_{\text{max}} / [1 + \exp((V_{1/2} - V)/k)]$, where G_{max} is the extrapolated maximum Na^+ conductance, *V* is the test voltage, $V_{1/2}$ is the half-activation voltage, and *k* is the slope factor. For Na_v steady-state inactivation, a voltage step to –20 mV for 20 ms was applied from a holding potential of –90 mV to preferentially activate I_{Na} after pre-pulse conditioning voltage steps of 300 ms in duration (ranging from –90 to +20 mV) in 5-mV increments. Steady-state inactivation curves were constructed by plotting the normalized peak current amplitude elicited during the test pulse as a function of the conditioning pre-pulse. A Boltzmann relationship, $I/I_{\text{max}} = (1 + \exp((V - V_{1/2})/k))^{-1}$ was used to fit the data where I_{max} is current elicited by the test pulse after a –90-mV prepulse; $V_{1/2}$ is half-inactivation voltage; *k* is the slope. Late Na_v current was measured at 150 ms during a 200 ms depolarizing pulse to –20 mV. The rate of decay of the transient Na_v current (τ) was obtained from a single exponential function, $I_{(t)} = I_{\text{Na}} \exp(-t/\tau) + I_{\text{SS}}$, where $I_{(t)}$ is the amplitude of the current at time *t*; I_{SS} is the steady-state current during a single voltage step.

In current clamp, action potential amplitude was measured as the peak voltage with respect to the baseline 10 ms before the peak of the action potential. The action potential duration was evaluated at half-amplitude. Evoked action potentials were elicited by injecting a depolarizing current from 0 pA to 300 pA for 600 ms duration with 10-pA increments.

Immunoprecipitation and Western blotting

Cerebella were isolated from two 5-week-old C57BL/6J mice and homogenized with a mortar and pestle in 8 ml of lysis buffer composed of 150 mM NaCl, 50 mM Tris-Cl, 1% Triton, and 1% sodium deoxycholate. Lysate was incubated on ice for 2 hr, passed through a 20g needle 20 times, and rocked end over end for 30 min at 4°C. The lysate was cleared of insoluble material by centrifugation at 4000 rcf at 4°C for 30 min followed by a second centrifugation at 17,100 rcf at 4°C

for 10 min. The lysate was preincubated with 30 μ l of Protein A/G (Santa Cruz Biotechnology) beads for 2 hr at 4°C. The beads were gently spun down at 0.4 rcf for 1 min to separate them from the lysate, which was then incubated with 20 μ g of either anti-FGF14 (NeuroMab) or non-immune mouse IgG (Santa Cruz Biotechnology) overnight at 4°C. In order to immunoprecipitate protein complexes, 30 μ l of Protein A/G beads were added and incubated with the lysate for 2 hr. Beads were then washed three times with lysis buffer followed by elution in 2 \times LDS Sample Buffer (Novex NuPage) plus 10 mM dithiothreitol. Protein samples were run on 8–16% Tris-glycine SDS page gels and transferred to PVDF membranes. Primary antibodies used were rabbit polyclonal anti Na_v1.6 from Millipore (1:200), anti- β -tubulin from Sigma (1:1000) as a loading control, and rabbit polyclonal anti-FGF14 (1:200), which was a kind gift from the Ornitz lab (Washington University, St. Louis). HEK293T cells on 100-mm plates were transfected with Lipofectamine 2000 (Invitrogen) when cells were at ~60% confluency with 9 μ g of Na_v1.6 and 3 μ g of FGF14b^{WT} or FGF14b^{RA}. Cells were washed with ice-cold PBS 60 hr after transfection, and cell lysates were prepared with the addition of lysis buffer containing 150 mM NaCl, 50 mM Tris-HCl, pH 7.5, 1% Triton with protease inhibitor (Roche). The pelleted cells were pipetted up and down 20 times with lysis buffer, incubated at 4°C for 1 hr and then centrifuged at 16,000 \times g for 10 min at 4°C. Immunoprecipitation was performed on 2 mg of lysate with 2 μ g of anti-FGF14 antibody (Neuromab). The samples were rocked gently at 4°C for 1 hr followed by addition of 30 μ l of protein A/G-agarose slurry. The samples were rotated overnight at 4°C and microcentrifuged at 7000 rpm for 2 min. After washing with lysis buffer three times, 40 μ l of loading buffer was added to the pellet, and protein was eluted from the beads by heating at 70°C for 20 min. The samples were subjected to NuPAGE 8–16% Bis-Tris gels (Invitrogen). The proteins were transferred to nitrocellulose membranes and subsequently immunoblotted with the anti-FGF14, anti-pan Na_v antibody, and anti-tubulin antibody.

Acknowledgements

We thank Dr Amanda H Lewis for insightful discussions. This work was supported by NIH R01 HL071165 and R01 HL112918 (GSP).

Additional information

Funding

Funder	Grant reference number	Author
National Heart, Lung, and Blood Institute	R01 HL071165	Geoffrey S Pitt
National Heart, Lung, and Blood Institute	R01 HL112918	Geoffrey S Pitt

The funder had no role in study design, data collection and interpretation, or the decision to submit the work for publication.

Author contributions

HY, Conception and design, Acquisition of data, Analysis and interpretation of data, Drafting or revising the article; JLP, CW, Acquisition of data, Analysis and interpretation of data, Drafting or revising the article; GSP, Conception and design, Analysis and interpretation of data, Drafting or revising the article

Author ORCIDs

Geoffrey S Pitt,  <http://orcid.org/0000-0003-2246-0289>

Ethics

Animal experimentation: This study was performed in strict accordance with the recommendations in the Guide for the Care and Use of Laboratory Animals of the National Institutes of Health. All of the animals were handled according to approved institutional animal care and use committee (IACUC) of Duke University for the protocol #A292-13-11.

Additional files

Major dataset

The following previously published dataset was used:

Author(s)	Year	Dataset title	Dataset ID and/or URL	Database, license, and accessibility information
Wang C, Chung BC, Yan H, Lee SY, Pitt GS	2012	Crystal structure of the C-terminus of voltage-gated sodium channel in complex with FGF13 and CaM	http://www.pdb.org/pdb/explore/explore.do?structureId=4DCK	Publicly available at RCSB Protein Data Bank.

References

- Aman TK**, Grieco-Calub TM, Chen C, Rusconi R, Slat EA, Isom LL, Raman IM. 2009. Regulation of persistent Na current by interactions between beta subunits of voltage-gated Na channels. *The Journal of Neuroscience* **29**:2027–2042. doi: [10.1523/JNEUROSCI.4531-08.2009](https://doi.org/10.1523/JNEUROSCI.4531-08.2009).
- Chen Y**, Yu FH, Sharp EM, Beacham D, Scheuer T, Catterall WA. 2008. Functional properties and differential neuromodulation of Na(v)1.6 channels. *Molecular and Cellular Neurosciences* **38**:607–615. doi: [10.1016/j.mcn.2008.05.009](https://doi.org/10.1016/j.mcn.2008.05.009).
- Coebergh JA**, Fransen van de Putte DE, Snoeck IN, Ruivenkamp C, van Haeringen A, Smit LM. 2013. A new variable phenotype in spinocerebellar ataxia 27 (SCA 27) caused by a deletion in the FGF14 gene. *European Journal of Paediatric Neurology* **18**:413–415. doi: [10.1016/j.ejpn.2013.10.006](https://doi.org/10.1016/j.ejpn.2013.10.006).
- Dalski A**, Atici J, Kreuz FR, Hellenbroich Y, Schwinger E, Zühlke C. 2005. Mutation analysis in the fibroblast growth factor 14 gene: frameshift mutation and polymorphisms in patients with inherited ataxias. *European Journal of Human Genetics* **13**:118–120. doi: [10.1038/sj.ejhg.5201286](https://doi.org/10.1038/sj.ejhg.5201286).
- Dover K**, Solinas S, D'Angelo E, Goldfarb M. 2010. Long-term inactivation particle for voltage-gated sodium channels. *The Journal of Physiology* **588**:3695–3711. doi: [10.1113/jphysiol.2010.192559](https://doi.org/10.1113/jphysiol.2010.192559).
- Goldfarb M**, Schoorlemmer J, Williams A, Diwakar S, Wang Q, Huang X, Giza J, Tchetchik D, Kelley K, Vega A, Matthews G, Rossi P, Ornitz DM, D'Angelo E. 2007. Fibroblast growth factor homologous factors control neuronal excitability through modulation of voltage-gated sodium channels. *Neuron* **55**:449–463. doi: [10.1016/j.neuron.2007.07.006](https://doi.org/10.1016/j.neuron.2007.07.006).
- Grieco TM**, Malhotra JD, Chen C, Isom LL, Raman IM. 2005. Open-channel block by the cytoplasmic tail of sodium channel beta4 as a mechanism for resurgent sodium current. *Neuron* **45**:233–244. doi: [10.1016/j.neuron.2004.12.035](https://doi.org/10.1016/j.neuron.2004.12.035).
- Gruol DL**, Franklin CL. 1987. Morphological and physiological differentiation of Purkinje neurons in cultures of rat cerebellum. *The Journal of Neuroscience* **7**:1271–1293.
- Hennessey JA**, Marcou CA, Wang C, Wei EQ, Wang C, Tester DJ, Torchio M, Dagradi F, Crotti L, Schwartz PJ, Ackerman MJ, Pitt GS. 2013. FGF12 is a candidate Brugada syndrome locus. *Heart Rhythm* **10**:1886–1894. doi: [10.1016/j.hrthm.2013.09.064](https://doi.org/10.1016/j.hrthm.2013.09.064).
- Hennessey JA**, Wei EQ, Pitt GS. 2013. Fibroblast growth factor homologous factors modulate cardiac calcium channels. *Circulation Research* **113**:381–388. doi: [10.1161/CIRCRESAHA.113.301215](https://doi.org/10.1161/CIRCRESAHA.113.301215).
- Kalume F**, Yu FH, Westenbroek RE, Scheuer T, Catterall WA. 2007. Reduced sodium current in Purkinje neurons from Nav1.1 mutant mice: implications for ataxia in severe myoclonic epilepsy in infancy. *The Journal of Neuroscience* **27**:11065–11074. doi: [10.1523/JNEUROSCI.2162-07.2007](https://doi.org/10.1523/JNEUROSCI.2162-07.2007).
- Khaliq ZM**, Gouwens NW, Raman IM. 2003. The contribution of resurgent sodium current to high-frequency firing in Purkinje neurons: an experimental and modeling study. *The Journal of Neuroscience* **23**:4899–4912.
- Laezza F**, Gerber BR, Lou JY, Kozel MA, Hartman H, Craig AM, Ornitz DM, Nerbonne JM. 2007. The FGF14(F145S) mutation disrupts the interaction of FGF14 with voltage-gated Na⁺ channels and impairs neuronal excitability. *The Journal of Neuroscience* **27**:12033–12044. doi: [10.1523/JNEUROSCI.2282-07.2007](https://doi.org/10.1523/JNEUROSCI.2282-07.2007).
- Laezza F**, Lampert A, Kozel MA, Gerber BR, Rush AM, Nerbonne JM, Waxman SG, Dib-Hajj SD, Ornitz DM. 2009. FGF14 N-terminal splice variants differentially modulate Nav1.2 and Nav1.6-encoded sodium channels. *Molecular and Cellular Neurosciences* **42**:90–101. doi: [10.1016/j.mcn.2009.05.007](https://doi.org/10.1016/j.mcn.2009.05.007).
- Liu C**, Dib-Hajj SD, Waxman SG. 2001. Fibroblast growth factor homologous factor 1B binds to the C terminus of the tetrodotoxin-resistant sodium channel rNav1.9a (NaN). *The Journal of Biological Chemistry* **276**:18925–18933. doi: [10.1074/jbc.M101606200](https://doi.org/10.1074/jbc.M101606200).
- Lou JY**, Laezza F, Gerber BR, Xiao M, Yamada KA, Hartmann H, Craig AM, Nerbonne JM, Ornitz DM. 2005. Fibroblast growth factor 14 is an intracellular modulator of voltage-gated sodium channels. *The Journal of Physiology* **569**:179–193. doi: [10.1113/jphysiol.2005.097220](https://doi.org/10.1113/jphysiol.2005.097220).
- Munoz-Sanjuan I**, Smallwood PM, Nathans J. 2000. Isoform diversity among fibroblast growth factor homologous factors is generated by alternative promoter usage and differential splicing. *The Journal of Biological Chemistry* **275**:2589–2597. doi: [10.1074/jbc.275.4.2589](https://doi.org/10.1074/jbc.275.4.2589).
- Raman IM**, Bean BP. 1999. Ionic currents underlying spontaneous action potentials in isolated cerebellar Purkinje neurons. *The Journal of Neuroscience* **19**:1663–1674.
- Raman IM**, Bean BP. 1997. Resurgent sodium current and action potential formation in dissociated cerebellar Purkinje neurons. *The Journal of Neuroscience* **17**:4517–4526.

- Raman IM**, Sprunger LK, Meisler MH, Bean BP. 1997. Altered subthreshold sodium currents and disrupted firing patterns in Purkinje neurons of Scn8a mutant mice. *Neuron* **19**:881–891. doi: [10.1016/S0896-6273\(00\)80969-1](https://doi.org/10.1016/S0896-6273(00)80969-1).
- Rush AM**, Wittmack EK, Tyrrell L, Black JA, Dib-Hajj SD, Waxman SG. 2006. Differential modulation of sodium channel Na(v)1.6 by two members of the fibroblast growth factor homologous factor 2 subfamily. *The European Journal of Neuroscience* **23**:2551–2562. doi: [10.1111/j.1460-9568.2006.04789.x](https://doi.org/10.1111/j.1460-9568.2006.04789.x).
- Shakkottai VG**, Xiao M, Xu L, Wong M, Nerbonne JM, Ornitz DM, Yamada KA. 2009. FGF14 regulates the intrinsic excitability of cerebellar Purkinje neurons. *Neurobiology of Disease* **33**:81–88. doi: [10.1016/j.nbd.2008.09.019](https://doi.org/10.1016/j.nbd.2008.09.019).
- Smallwood PM**, Munoz-Sanjuan I, Tong P, Macke JP, Hendry SH, Gilbert DJ, Copeland NG, Jenkins NA, Nathans J. 1996. Fibroblast growth factor (FGF) homologous factors: new members of the FGF family implicated in nervous system development. *Proceedings of the National Academy of Sciences of USA* **93**:9850–9857. doi: [10.1073/pnas.93.18.9850](https://doi.org/10.1073/pnas.93.18.9850).
- van Swieten JC**, Brusse E, de Graaf BM, Krieger E, van de Graaf R, de Koning I, Maat-Kievit A, Leegwater P, Dooijes D, Oostra BA, Heutink P. 2003. A mutation in the fibroblast growth factor 14 gene is associated with Autosomal dominant Cerebral ataxia. *The American Journal of Human Genetics* **72**:191–199. doi: [10.1086/345488](https://doi.org/10.1086/345488).
- Wang C**, Chung BC, Yan H, Lee SY, Pitt GS. 2012. Crystal structure of the ternary complex of a NaV C-terminal domain, a fibroblast growth factor homologous factor, and calmodulin. *Structure* **20**:1167–1176. doi: [10.1016/j.str.2012.05.001](https://doi.org/10.1016/j.str.2012.05.001).
- Wang C**, Hennessey JA, Kirkton RD, Wang C, Graham V, Puranam RS, Rosenberg PB, Bursac N, Pitt GS. 2011. Fibroblast growth factor homologous factor 13 regulates Na⁺ channels and conduction velocity in murine hearts. *Circulation Research* **109**:775–782. doi: [10.1161/CIRCRESAHA.111.247957](https://doi.org/10.1161/CIRCRESAHA.111.247957).
- Wang Q**, Bardgett ME, Wong M, Wozniak DF, Lou J, McNeil BD, Chen C, Nardi A, Reid DC, Yamada K, Ornitz DM. 2002. Ataxia and paroxysmal dyskinesia in mice lacking axonally transported FGF14. *Neuron* **35**:25–38. doi: [10.1016/S0896-6273\(02\)00744-4](https://doi.org/10.1016/S0896-6273(02)00744-4).
- Wang Q**, McEwen DG, Ornitz DM. 2000. Subcellular and developmental expression of alternatively spliced forms of fibroblast growth factor 14. *Mechanisms of Development* **90**:283–287. doi: [10.1016/S0925-4773\(99\)00241-5](https://doi.org/10.1016/S0925-4773(99)00241-5).
- Yan H**, Pablo JL, Pitt GS. 2013. FGF14 regulates presynaptic Ca²⁺ channels and synaptic transmission. *Cell Reports* **4**:66–75. doi: [10.1016/j.celrep.2013.06.012](https://doi.org/10.1016/j.celrep.2013.06.012).